

Elastic properties of permanently densified silica: A Raman, Brillouin light, and x-ray scattering study

M. Zanatta,¹ G. Baldi,^{2,3} S. Caponi,^{1,2} A. Fontana,^{1,2} E. Gilioli,⁴ M. Krish,³ C. Masciovecchio,^{2,5} G. Monaco,^{2,3} L. Orsinger,³ F. Rossi,^{1,2} G. Ruocco,^{2,6} and R. Verbeni³

¹*Dipartimento di Fisica, Università di Trento, 38050 Povo, Trento, Italy*

²*IPCF-CNR Unità Organizzativa di Supporto c/o Università di Roma "La Sapienza," 00185 Roma, Italy*

³*European Synchrotron Radiation Facility, BP 220, 38043 Grenoble, France*

⁴*Istituto dei Materiali per Elettronica e Magnetismo (IMEM), CNR, Area delle Scienze, 43100 Parma, Italy*

⁵*Sincrotrone di Trieste, Strada Statale 14 km 163.5, 34012 Basovizza, Trieste, Italy*

⁶*Dipartimento di Fisica, Università di Roma "La Sapienza," 00185 Roma, Italy*

(Received 22 March 2010; revised manuscript received 1 June 2010; published 17 June 2010)

Raman, Brillouin light, and x-ray scattering measurements have been carried out to characterize the low-frequency vibrational dynamics of the SiO₂ glass as function of its density. The obtained results demonstrate that while the distribution of the low-frequency states in the boson peak range is conserved under densification, these modes do not shift as a function of density as the acoustic modes do. The clear difference between the behavior of the vibrational states in the Boson peak range and that of the acoustic modes, could be explained considering the contribution of specific nonacoustic modes (tetrahedra rotation).

DOI: [10.1103/PhysRevB.81.212201](https://doi.org/10.1103/PhysRevB.81.212201)

PACS number(s): 63.50.Lm, 78.30.Ly, 78.35.+c, 78.70.Ck

In glasses, sound waves with wavelengths much larger than the interparticles separation experience a continuum medium, and are basically plane waves. Increasing the wave vector q up to values comparable to the inverse of the interparticles separation, the disorder starts to play a role, and the sound waves are not any more neither simple plane waves nor eigenstates of the dynamical matrix of the system. The characteristics of these excitations is still a debated issue¹⁻³ and the comprehension of their nature is related to the study on the origin of the boson peak, the well known excess of modes in the vibrational density of states $g(\omega)$ of amorphous materials.^{1,4,5} The boson peak (BP) appears as a large bump in the reduced density of states $g(\omega)/\omega^2$ (Ref. 6) and, despite of the large theoretical and experimental efforts,^{4,6-14} its explanation is still a debated topic.

On the experimental side, strong interest has been addressed to the connection between the variation of the elastic properties of the medium, i.e., the Debye frequency ω_{DB} , and the features of the BP. This comparison involves the BP frequency ω_{BP} (the frequency of the peak maximum) and its intensity. In particular, the boson peak has been studied as a function of temperature,¹⁵⁻¹⁷ aging of the systems,¹⁸ density,¹⁹⁻²⁵ and during a chemical vitrification process.²⁶ In all the systems investigated so far a shift toward higher frequencies of ω_{BP} and a decrease in the BP intensity takes place along with a hardening of the elastic medium, i.e., an increase of the sound velocity and/or of the density. Nevertheless, a quantitative comparison of ω_{DB} and ω_{BP} leads to different and sometimes contrasting results. Indeed, the evolution of the BP on some systems as sodium silicated glasses as a function of temperature,¹⁵ density,²² varying the sample preparation,¹⁸ or in an epoxy-amine mixture during chemical vitrification,²⁶ can be fully explained with elastic medium modifications suggesting a simple law for the BP scaling. Conversely, in densified systems as GeO₂ (Ref. 25) and polymeric glasses^{23,24} as a function of the applied pressure, the BP shift is faster than the ω_{DB} modifications. These findings

suggest that the elastic medium explanation does not cover the full story.

The present work reports on a study on a prototypical glass, permanently densified v -SiO₂. Densified v -SiO₂ has been investigated in the past by several research groups;^{27,28} here we show the existence of a scaling law for the BP as a function of density and we demonstrate that the related scaling coefficient has a stronger dependence on density than the Debye frequency. This result is based on a detailed characterization of the elastic medium by means of Brillouin light scattering (BLS) and inelastic x-ray scattering (IXS) measurements, respectively, in the gigahertz and terahertz frequency range. The intensity and the spectral information on the BP have been obtained through Raman scattering measurements.

The samples were obtained from a commercial-grade Spectrosil block glass, v -SiO₂, purchased from SILO (Florence). The starting block was drilled in cylindrical pieces of 4 mm diameter and 4 mm length, which were densified using a high-temperature high-pressure multi-anvil apparatus²⁹ at pressures of 2, 4, and 6 GPa. The samples were heated at $T=500$ °C for 10 min with a heating rate of 50 °C/min; the pressure was released after quenching. The final products were homogeneous and permanently densified. The densities, ρ , were measured by the Archimedes method using ethanol as immersion fluid, and yielded the values of 2.210 ± 0.005 g/cm³, 2.255 ± 0.005 g/cm³, 2.406 ± 0.005 g/cm³. At the highest pressure, we achieved 9.5% densification with respect to the normal one. In the following, we refer to the samples using the densification pressure.

The Raman scattering experiments were performed using a Jobin-Yvon U1000 double monochromator both in vertical-vertical (VV) and horizontal-vertical (HV) polarization configurations. The incident light was the 514.5 nm line of an Argon laser. The spectra were collected in a wide frequency range (-300 – 1300 cm⁻¹) with different frequency resolu-

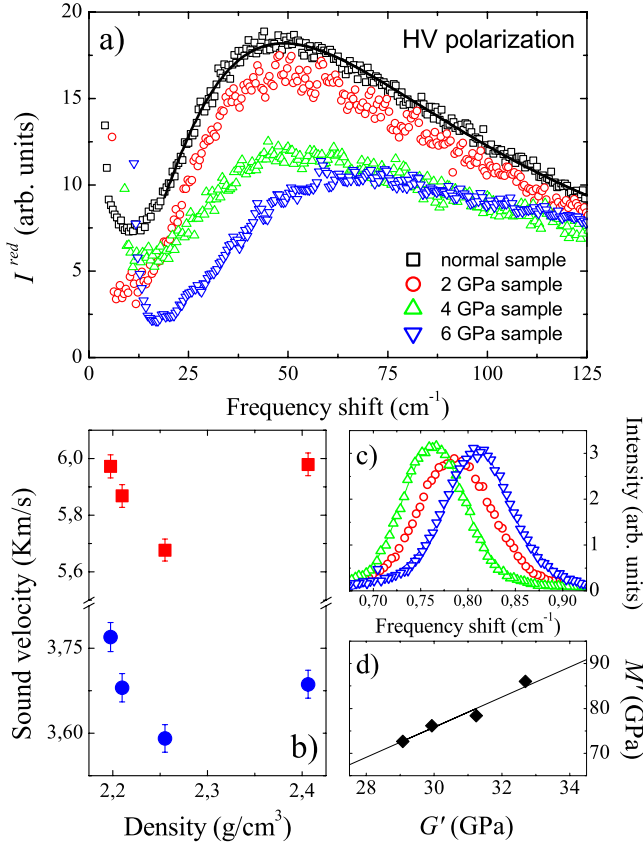


FIG. 1. (Color online) (a) reduced Raman spectra for the normal and densified samples as reported in the legend; the continuous line represents the fit using a log-normal function defined as $I(\omega) \propto \exp\left[-\frac{(\ln(\omega/\omega_{BP}))^2}{2\Gamma^2}\right]$, where Γ is the BP width; (b) longitudinal (squares) and transverse (dots) sound velocities as a function of density; (c) longitudinal Brillouin lines (symbols as in a); (d) real part of the longitudinal modulus $M' = \rho v_L^2$ vs shear modulus $G' = \rho v_T^2$ (black diamonds) and linear fit using the Cauchy-like relation $M' = A + BG'$ (black line).

tions; for the low-frequency spectra the resolution was fixed to about 2 cm⁻¹. The finally obtained spectra are consistent with those already published in the literature.²⁷ In order to compare spectra corresponding to different densities they were normalized to the same total measured area. In the case of first-order Raman scattering, for a Stokes process, the intensity I_R is proportional to the density of states $g(\omega)$, namely,

$$I_R(\omega) = C(\omega)g(\omega)\frac{[n(\omega) + 1]}{\omega}, \quad (1)$$

where $C(\omega)$ is the light to vibration coupling function and $n(\omega)$ is the Bose factor. The reduced Raman intensity is defined as

$$I^{red}(\omega) = \frac{I_R(\omega)}{[n(\omega) + 1]\omega} = C(\omega)\frac{g(\omega)}{\omega^2}, \quad (2)$$

The low-frequency part of the HV spectra are shown in Fig. 1(a) in terms of reduced Raman intensity. The BP maximum shifts toward higher frequencies and its intensity decreases

on increasing the density. In order to accurately determine ω_{BP} , we fitted the Raman spectra using a log-normal function as indicated in Fig. 1(a).

To compare on a quantitative basis the changes in the BP with the elastic medium transformation, we measured the sound velocity in the same samples by BLS measurements. Experiments were carried out using a laser with $\lambda = 514.5$ nm and a SOPRA double-pass monochromator as spectrometer. The 90° scattering geometry with no polarization analysis of the scattered light allowed us to measure both the longitudinal and the transverse acoustic modes in the same spectrum. In Fig. 1(c) the longitudinal Brillouin peaks are shown for the densified samples. We notice that the frequency of the peaks is not linearly dependent on the density. The refractive index, necessary to determine the sound speed, was measured using a prism coupling technique at the same wavelength. The resulting sound velocities values are shown in Fig. 1(b). They are consistent with previous measurements as a function of pressure.³⁰ While the BP shifts in a continuous way on increasing density, the sound velocity does not follow the same behavior, hence the elastic medium transformation *cannot* explain the BP shift.

As already pointed out in Refs. 15 and 26, the presence of anharmonicity and/or relaxations could affect the low-frequency sound velocity values. Therefore, to obtain the appropriate Debye frequency to be compared to ω_{BP} , it is necessary to measure the sound velocity also in the high frequency regime. For this reason, IXS experiments were performed on the 6 GPa densified sample at the beam line ID28 of the European Synchrotron Radiation Facility. The experimental set-up yielded an instrumental energy resolution of 1.4 meV. The IXS spectra were taken at several exchanged q values in the range from 1.15 to 2.36 nm⁻¹. The measurements were performed at $T = 573$ K in order to increase the population of the acoustic excitations and therefore improve the statistical accuracy of the data. As an example, Fig. 2(a) shows the experimental spectrum corresponding to $q = 1.45$ nm⁻¹ together with the line shapes of the main fitting components: a delta function for the elastic line and a damped harmonic oscillator function for the inelastic component, both convoluted with the instrumental resolution. The energy gain part of the Brillouin doublet, at selected q values together with the best fitting line shape, is shown in Fig. 2(b). These spectra have been obtained after subtracting the best fitting elastic component from the measured spectra. The dispersion curve is displayed in Fig. 2(c). The dashed line is the extrapolation of the low-frequency sound velocity measured by BLS. IXS and BLS sound velocities are in good agreement, even if the terahertz data are slightly lower than the gigahertz ones. This small difference could be ascribed to the presence of a softening of the modes in the low- q region, around the BP frequency, as it has been recently shown in other glassy systems.²

In order to compare the elastic medium modifications with the BP changes as a function of system density, we need to evaluate the Debye frequency,

$$\omega_{DB}^3 = 6\pi^2 n \langle v \rangle^3 = 18\pi^2 n \left[\frac{1}{v_L^3} + \frac{2}{v_T^3} \right]^{-1}, \quad (3)$$

where n is the number density and $\langle v \rangle$ the Debye velocity. For the BLS data, this calculation is straightforward because

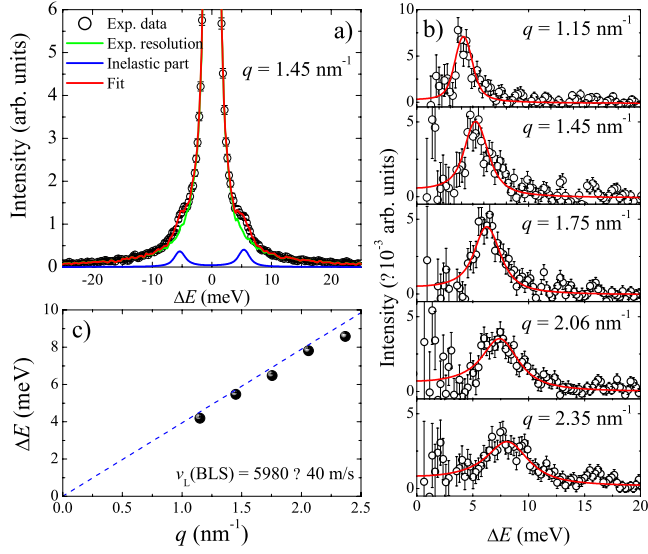


FIG. 2. (Color online) (a) representative IXS spectrum on the 6 GPa sample (open circles) at $T=573$ K and $q=1.45$ nm $^{-1}$. The measured instrumental resolution is also reported (green line). The red line is the best fit of data, while the blue line is the inelastic contribution. (b) The inelastic components plotted after subtracting the elastic line for several q -values. (c) Dispersion curve for 6 GPa sample (full circles). The dashed line is the extrapolation of the BLS sound velocity.

we measured both the longitudinal and the transverse sound velocities, v_L and v_T . The value of $\langle v \rangle$ in the purely elastic limit is obtained from the IXS data, which, however, provide only the longitudinal sound velocity. The transverse one can be estimated using the Cauchy relation $M' = A + BG'$ connecting $M' = \rho v_L^2$, the real part of the longitudinal elastic modulus and $G' = \rho v_T^2$ the transverse one. This relation has been recently found to hold for a great variety of systems at all frequencies³² with $B \sim 3$ and A a system dependent constant. In Fig. 1(d) are reported G' and M' , calculated using BLS sound velocity values. Data shows again a linear behavior with a slope $B = 3.3 \pm 0.7$. This confirms the applicability of the Cauchy relation and allows the determination of the high frequency transverse sound velocity and then the appropriate Debye frequency.

In order to check whether the shift of the Boson Peak can be totally ascribed to changes in the elastic constants, we can compare the dependence of ω_{BP} and ω_{DB} on the same plot, Fig. 3(a). Data are normalized to their normal density value. The high frequency sound velocity of the normal silica glass is taken from Ref. 31. In the same plot we also show the BP position obtained by means of inelastic neutron scattering.²⁸ Raman and neutron data show the same trend, indicating that the Raman coupling function does not induce strong modifications in the density behavior of ω_{BP} . Figure 3(a) shows that the density dependence of ω_{BP} and ω_{DB} is roughly linear, though with slopes about one order of magnitude different. This result clearly demonstrates that the elastic medium transformations cannot account for the BP shift.

Now we analyze the shape of the BP as a function of the sample densification. In particular, we have rescaled the x axis of the Raman spectra by squeezing the frequency as ν

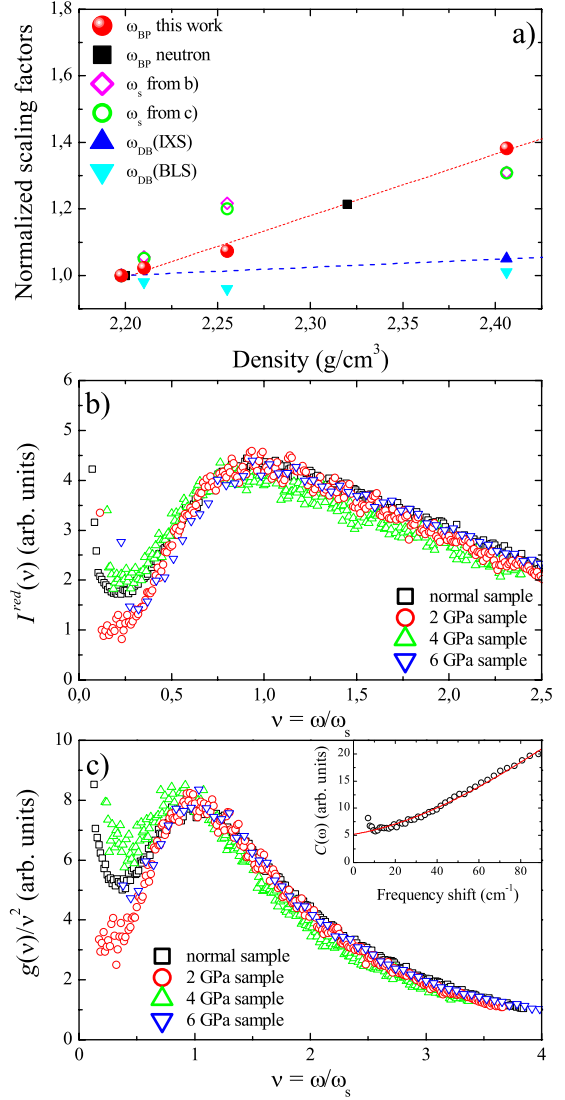


FIG. 3. (Color online) (a) red bullets correspond to the Boson Peak frequency as function of density obtained from Raman spectra; black squares to the corresponding data obtained using neutron scattering (Ref. 28). Open diamonds and circles: maximum of I^{red} and $g(\omega)/\omega^2$, obtained as discussed in the text. Cyan down-triangles: Debye frequency calculated using BLS sound velocities; blue up-triangles: Debye frequency calculated for the ambient conditions and the 6 GPa samples using the IXS sound velocity. (b) Master curve of the Boson Peak for the reduced Raman intensity obtained as discussed in the text. (c) Master curve of $g(\omega)/\omega^2$ obtained as discussed in the text. In the inset the experimental $C(\omega)$ (circles) obtained from the ratio of Raman and neutron scattering data (Ref. 34) is reported together with its fit (continuous line).

$= \omega/\omega_s$. Taking into account the proper normalization of the density of states $g(\nu)d\nu = g(\omega)d\omega$, resulting from the change of variable, and assuming that $C(\omega)$ in Eq. (2) is proportional to ω in the BP region (as it has been shown for several glasses^{33–35}), we obtain the rescaled intensity as¹⁷

$$I(\nu) = I^{red}(\omega) \times \omega_s^2, \quad (4)$$

using ω_s as a fit parameter. The so-squeezed spectra are shown in Fig. 3(b): the spectra rescale one on top of the

other. A master curve, whose existence is also expected by theoretical predictions,¹² is obtained. The existence of this master curve demonstrates that the decrease of the BP intensity is only an apparent effect due to its shift with density. As a matter of fact the BP raises from a plateau in $g(\omega)$ when divided by ω^2 . When it shifts upwards it becomes more and more suppressed by this division. The same result is reached if the scaling is performed on $g(\omega)/\omega^2$. In order to do this, we divide Eq. (2) by the experimental coupling function $C(\omega)$ measured in nondensified silica from the ratio of Raman and neutron scattering data.³⁴ We assume that $C(\omega)$ does not change with densification. This hypothesis is supported by the results obtained in densified v -GeO₂. It has been demonstrated that in a similar densification range, the coupling function does not depend on the sample density.²⁵ Hence, the reduced density of states rescales as

$$g(\nu)/\nu^2 = [g(\omega)/\omega^2] \times \omega_s^3. \quad (5)$$

Open diamonds in Fig. 3(a) correspond to the ω_s squeezing factors used in Fig. 3(b) and open circles correspond to the ω_s values used in Fig. 3(c). In both cases we find the same behavior for the scaling factor ω_s . This gives strong evidence

of the equivalence of the two methods. Moreover, it can be seen from Fig. 3(a) that the squeezing factors ω_s —despite of being more scattered—show a comparable density dependence as ω_{BP} . The difference is presumably due to the fact that it is always difficult to obtain an absolute Raman intensity. Nevertheless the overall obtained result of Fig. 3 seems quite clear.

To conclude, we investigated the vibrational dynamics of permanently densified vitreous silica by Raman, Brillouin light, and x-ray scattering. We found: (a) the scaling of the BP with the continuum medium properties represented by the Debye frequency is not a universal feature of disordered materials; (b) the existence of a scaling law for the BP spectral shape is here verified in a case where the boson peak position changes by 40%, and it seems a far more general result. Therefore the distribution of the low-frequency states in the boson peak range is conserved under densification, and these modes do not shift as a function of density as the acoustic modes do. This is likely related to the fact that in v -SiO₂ the boson peak has a strong contribution from specific nonacoustic modes (tetrahedra rotations).³⁶ The present results indicate that their mode Grüneisen parameters are as well distinctively different from that of the acoustic modes.

- ¹M. Foret *et al.*, *Phys. Rev. B* **66**, 024204 (2002); B. Rufflé *et al.*, *Phys. Rev. Lett.* **96**, 045502 (2006).
- ²G. Monaco and V. M. Giordano, *Proc. Natl. Acad. Sci. U.S.A.* **106**, 3659 (2009); G. Monaco and S. Mossa, *ibid.* **106**, 16907 (2009); G. Baldi *et al.*, *Phys. Rev. Lett.* **104**, 195501 (2010).
- ³G. Ruocco *et al.*, *Phys. Rev. Lett.* **98**, 079601 (2007).
- ⁴B. Rufflé *et al.*, *Phys. Rev. Lett.* **100**, 015501 (2008).
- ⁵C. Masciovecchio *et al.*, *Phys. Rev. Lett.* **97**, 035501 (2006).
- ⁶U. Buchenau *et al.*, *J. Phys.: Condens. Matter* **19**, 205106 (2007).
- ⁷H. Shintani and H. Tanaka, *Nature Mater.* **7**, 870 (2008).
- ⁸A. Fontana *et al.*, *Phys. Rev. Lett.* **78**, 1078 (1997).
- ⁹S. N. Taraskin *et al.*, *Phys. Rev. Lett.* **86**, 1255 (2001).
- ¹⁰W. Götze and M. R. Mayr, *Phys. Rev. E* **61**, 587 (2000).
- ¹¹D. A. Parshin *et al.*, *Phys. Rev. B* **76**, 064206 (2007).
- ¹²T. S. Grigera *et al.*, *Nature (London)* **422**, 289 (2003).
- ¹³B. Schmid and W. Schirmacher, *Phys. Rev. Lett.* **100**, 137402 (2008).
- ¹⁴B. Ruzicka *et al.*, *Phys. Rev. B* **69**, 100201(R) (2004).
- ¹⁵G. Baldi *et al.*, *Phys. Rev. Lett.* **102**, 195502 (2009).
- ¹⁶B. Rufflé *et al.*, *Phys. Rev. Lett.* **104**, 067402 (2010).

- ¹⁷S. Caponi *et al.*, *Phys. Rev. B* **76**, 092201 (2007).
- ¹⁸A. Monaco *et al.*, *Phys. Rev. Lett.* **96**, 205502 (2006).
- ¹⁹O. Pilla *et al.*, *J. Phys.: Condens. Matter* **15**, S995 (2003).
- ²⁰O. Pilla *et al.*, *J. Phys.: Condens. Matter* **16**, 8519 (2004).
- ²¹V. L. Gurevich *et al.*, *Phys. Rev. B* **71**, 014209 (2005).
- ²²A. Monaco *et al.*, *Phys. Rev. Lett.* **97**, 135501 (2006).
- ²³K. Niss *et al.*, *Phys. Rev. Lett.* **99**, 055502 (2007).
- ²⁴L. Hong *et al.*, *Phys. Rev. B* **78**, 134201 (2008).
- ²⁵L. Orsingher *et al.*, *J. Chem. Phys.* **132**, 124508 (2010).
- ²⁶S. Caponi *et al.*, *Phys. Rev. Lett.* **102**, 027402 (2009).
- ²⁷S. Sugai and A. Onodera, *Phys. Rev. Lett.* **77**, 4210 (1996).
- ²⁸Y. Inamura *et al.*, *Physica B* **284-288**, 1157 (2000).
- ²⁹L. Orsingher *et al.*, *Philos. Mag.* **88**, 3907 (2008).
- ³⁰C. Zha *et al.*, *Phys. Rev. B* **50**, 13105 (1994).
- ³¹G. Baldi *et al.* (unpublished).
- ³²D. Fioretto *et al.*, *J. Chem. Phys.* **128**, 214502 (2008).
- ³³A. P. Sokolov *et al.*, *Phys. Rev. B* **52**, R9815 (1995).
- ³⁴A. Fontana *et al.*, *EPL* **47**, 56 (1999).
- ³⁵A. Fontana *et al.*, *J. Phys.: Condens. Matter* **19**, 205145 (2007).
- ³⁶E. Fabiani *et al.*, *J. Chem. Phys.* **128**, 244507 (2008).